Journal of Cleaner Production 319 (2021) 128788

Contents lists available at ScienceDirect

Journal of Cleaner Production

journal homepage: www.elsevier.com/locate/jclepro

Durability and surface properties of low-noise pavements with recycled concrete aggregates

Peter Mikhailenko [a,*], Zhengyin Piao [a,b], Muhammad Rafiq Kakar [a,c], Moises Bueno [a], Lily D. Poulikakos [a]

[a] Empa, Swiss Federal Laboratories for Materials Science and Technology, Laboratory for Concrete and Asphalt, Dübendorf, Switzerland
[b] ETH Zurich, Swiss Federal Institute of Technology Zurich, Institute of Environmental Engineering, Ecological Systems Design, Zurich, Switzerland
[c] Bern University of Appllied Sciences, Department of Architecture, Wood and Civil Engineering, Bern, Switzerland

ARTICLE INFO

Handling editor Zhen Leng

Keywords:
Recycled concrete aggregates (RCA)
Semi-dense asphalt (SDA)
Semi-circular bending (SCB)
Rutting
Surface texture

ABSTRACT

In order to improve the sustainability of the low-noise Semi-Dense Asphalt (SDA), the aggregate fractions were replaced by recycled concrete aggregates (RCA), an abundant construction waste. The aggregate replacement was conducted by fractions of 2/4 and 0.125/2 mm corresponding to the 2/4 mm (coarse), 0.063/4 mm (sand) fractions of the control virgin aggregates, at about 15% replacement by volume of the control mixture for each fraction. Additionally, RCA filler replaced the control filler entirely, bringing the replacement level to over 20% of the total mixture. The binder was added at the same amount as the control binder and +0.5%, with additional binder compensating for the estimated increase in binder absorption in RCA. The wheel track rutting test at 60 °C indicated marginally improved performance with RCA sand replacement. However, low temperature semi-circular bending (SCB) test at 0 °C showed that there is a 10% reduction in cracking resistance using RCA coarse and 20% for RCA sand. The laser texture scanning indicated a small reduction in the texture level for the RCA samples before wheel tracking, and very similar texture profiles with the control after the wearing of the samples, indicating no significant effect in non-acoustic noise reduction properties. This study suggests that the use of RCA fractions in porous SDA surface mixtures is possible with particular attention to mixture optimization to improve rutting performance.

1. Introduction

Construction and demolition waste is the most prevalent type of waste in the world (Gálvez-Martos et al., 2018), with recycled concrete making up a majority of this (Monier et al., 2011). The latter is often recycled in concrete as Recycled Concrete Aggregates (RCA) (Poulikakos et al., 2017), but the quality of the new concrete is limited (Bogas et al., 2016) due to the durability issues with RCA (Mills-Beale and You, 2010; Ossa et al., 2016). Another common RCA destination is various types of granular fill (Soleimanbeigi et al., 2015; Yaghoubi et al., 2018), which account for 40% of the yearly 2.7 billion ton EU aggregate demand (UEPG, 2018), and are thus suitable for recycling large amounts. However, when these granular materials are used in road construction (Riviera et al., 2014), it is desirable to have mostly coarse aggregates (>4 mm) due to the engineering requirements (Birgisson and Roberson, 2000). Finding an appropriate use for the finer RCA fractions, would be very beneficial for reuse in this waste cycle.

A potential destination for these aggregates is asphalt pavements. Asphalt consumes a large amount of aggregates, as it is the 2nd most commonly manufactured construction material in the world after concrete, and accounts for 10% of the EU aggregate use (UEPG, 2018). Asphalt mixtures also do not suffer from the same chemical based durability issues (Sadati and Khayat, 2018), which result in high RCA contents being unsuitable for many Portland cement concretes. Semi-dense asphalt (SDA) surface mixtures, commonly used in Switzerland (SN 640436), is produced to have similar noise reduction properties to porous asphalt (PA) (Steiner et al., 2018), while being somewhat more durable (Pérez et al., 2010). They typically have an air voids content of 10–18% and a maximum aggregate size of 4–8 mm (Poulikakos et al., 2019). Furthermore, SDA is known for good skid resistance properties, while having issues with raveling (Jacobs et al., 2015). Due to the shorter service life compared to the conventional asphalt surface course, SDA would consume more aggregates within the same period of time. Thus, RCA replacement in asphalt would have the

* Corresponding author. Swiss Federal Laboratories for Material Science and Technology, Überlandstrasse 129, 8600, Dübendorf, Switzerland.
E-mail address: peter.mikhailenko@empa.ch (P. Mikhailenko).

https://doi.org/10.1016/j.jclepro.2021.128788
Received 1 April 2021; Received in revised form 30 July 2021; Accepted 21 August 2021
Available online 25 August 2021

additional benefit of being able to reduce the consumption of virgin aggregates which need to be mined and processed.

As shown in Table 1, a number of studies have looked at the effects of RCA replacement (Albayati et al., 2018) in asphalt mixtures (Nejad et al., 2013; Pasandín and Pérez, 2017), with varied results (Radević et al., 2017; Wu et al., 2017). Common to these studies is that RCA was replaced in bulk and that it absorbed a significant amount of binder (Hou et al., 2014) from the coarse aggregates (Pasetto et al., 2020; Wu et al., 2013). This can be addressed through adding more binder or employing pretreatment (Al-Bayati et al., 2016), but at the expense of making the mixture more costly. Performance-wise, mixtures with RCA are more crack prone (Hou et al., 2014; Prakash Giri et al., 2020) due to the presence of cement paste around the concrete aggregates (Leemann and Loser, 2019). Portland cement paste is generally weaker and more porous (Chen and Wong, 2013; Wu et al., 2013) than the natural or crushed stone used in building materials. This is due to the formation of weaker crystals during the hydration process and is especially the case near the aggregate, where the interfacial transition zone is found (Ye et al., 2012). There have been some attempts to overcome these shortcomings in the aggregates themselves. The removal of the cement paste from the RCA particles through acid-treatment or heating is an option (Al-Bayati et al., 2016). However, this can often result in rounded aggregates, not suitable for asphalt mixtures (Castillo et al., 2018).

Recent studies replacing virgin aggregates with RCA by fraction have found promising results. RCA replacement in dense asphalt produced good results in Marshall stability and permanent deformation for only the fine (0.075/4.75 mm) and filler RCA replacement, while coarse RCA (4.75/19 mm) produced the opposite result. It was also noted that the aggregate size distribution trended to smaller sizes due to fragmentation in mixing (Arabani et al., 2013). A study using similar coarse and fine RCA replacement found reduced water sensitivity and low-temperature cracking resistance (Wu et al., 2013). Replacement of coarse (2/4 mm) and fine RCA by mass in SDA has produced similar results with water sensitivity when replacement is limited to below 20% by total aggregate and slightly improved the rutting resistance. However, compactibility and fracture susceptibility were issues due to the lower density and higher brittleness of RCA, respectively. Full replacement of the filler fraction by RCA filler was found to result in the same mixture performance compared to natural aggregates, which was still a desirable outcome given the filler is a waste material replacing a mined one (Mikhailenko et al., 2020a). A previous study showed RCA filler replacement led to the improvement of rutting and fatigue resistance of dense asphalt (Chen et al., 2011), with similar results found from other types of cement based powders (Orešković et al., 2019). A recent review paper has shown that RCA can be used in asphalt mixtures with good laboratory performance although the technical readiness level (TRL) was relatively low, indicating little in-situ experience and the need to establish trust and removing barriers to facilitate the use of this kind of alternative road material (Piao et al., 2021).

RCA replacement by fractions (coarse, sand and filler) in asphalt mixtures has been shown potential to be a way to find a destination for large amounts of construction waste, but studies examining this approach have been infrequent, and aspects such as low-temperature cracking and surface texture have not been looked at. Furthermore, this has been seldom applied to high value porous pavements like semi-dense asphalt (SDA) or the performance optimized by specifying the RCA fractions replacement. Finally, the effects of RCA on asphalt texture, important for noise reduction, before and after wearing have not been studies to date.

This study will examine two types of SDA mixtures with around 20% RCA replacement by volume. The mixtures will be evaluated for volumetrics, compactibility, rutting, cracking resistance and surface texture properties. This research, which builds on the work of some recent results on RCA replacement as part of a larger project on green low-noise pavements, further evaluates the performance viability of fraction-based RCA replacement in porous asphalt mixtures.

Table 1
Peer-reviewed journal studies employing construction waste as aggregate replacement in asphalt mixtures (2016–21).

Study	Author (s)	Year	Aggregated Use	Testing
Use of recycled construction and demolition waste (CDW) aggregates: a sustainable alternative for the pavement construction industry	Ossa et al.	2016	C&D waste in HMA at 10–40% replacement.	Water sensitivity, rutting.
Key performance properties of asphalt mixtures with recycled concrete aggregate from low strength concrete	Zhang et al.	2016	RCA from low-strength concrete in HMA at 30, 50, 75% replacement.	Low-temperature cracking, water sensitivity, freeze-thaw.
Fatigue performance of bituminous mixtures made with recycled concrete aggregates and waste tire rubber	Pasandin & Pérez	2017	RCA (35, 42% replacement) and rubber in HMA.	Fatigue.
Effects of recycled concrete aggregate on stiffness and rutting resistance of asphalt concrete	Radević et al.	2017	RCA replacement fractions (15–45%).	Stiffness, rutting.
Investigation of effectiveness of prediction of fatigue life for hot mix asphalt blended with recycled concrete aggregate using monotonic fracture testing	Wu et al.	2017	RCA replacement at 20–100%.	Fatigue.
Laboratory Evaluation of Hot Asphalt Concrete Properties with Cuban Recycled Concrete Aggregates	Acosta Alvarez et al.	2018	RCA in HMA at 40% replacement.	Stability, stiffness, dynamic modulus.
A sustainable pavement concrete using warm mix asphalt and hydrated lime treated recycled concrete aggregates	Albayati et al.	2018	Hydrated lime treated RCA in warm-mix.	Flow, stability, resilient modulus, rutting, IT strength, fatigue.
Evaluation of recycled concrete aggregate in asphalt mixes	El-Tahan et al.	2018	100% RCA replacement in HMA.	Stability, IT strength, abrasion loss.
Adhesion between Asphalt and Recycled	Hou et al.	2018	RCA replacement at 30% in HMA.	Binder adhesion properties, water

(continued on next page)

Table 1 (*continued*)

Study	Author (s)	Year	Aggregated Use	Testing
Concrete Aggregate and Its Impact on the Properties of Asphalt Mixture				sensitivity, fatigue.
Evaluation of the double coated recycled concrete aggregates for hot mix asphalt	Kareem et al.	2018	Double-coated RCA replacement at 20, 40 and 60%.	Water sensitivity, resilient modulus.
Mechanical Behavior of Hot-Mix Asphalt Made with Recycled Concrete Aggregates from Construction and Demolition Waste: A Design of Experiments Approach	Galan et al.	2019	C&D waste aggregates replacement at 20, 40 and 60%.	Water sensitivity, IT strength.
Performance of hot-mix asphalt produced with double coated recycled concrete aggregates	Kareem et al.	2019	Cement-slag coated RCA at 20, 40 and 60% replacement.	Flow, fatigue, rutting, dynamic modulus.
Potential of recycled concrete aggregate pretreated with waste cooking oil residue for hot mix asphalt	Ma at al.	2019	Waste cooking oil treated RCA in HMA replaced at 20% fine and 40% coarse.	Cracking, fatigue, dynamic modulus, water sensitivity, microscopy.
Laboratory Evaluation of Hot Asphalt Concrete Properties with Cuban Recycled Concrete Aggregates	Acosta Álvarez et al.	2020	RCA in HMA at 20, 40, 60, 80% replacement.	Stability, flow, stiffness, water sensitivity, rutting.
Performance Enhancement of Permeable Asphalt Mixtures With Recycled Aggregate for Concrete Pavement Application	Lei et al.	2020	Treated RCA in porous asphalt replaced at 30, 70 and 100% replacement	Stability, abrasion, permeability.
Incorporation of recycled concrete aggregate (RCA) fractions in semi-dense asphalt (SDA) pavements: Volumetrics, durability and mechanical properties	Mikhailenko et al.	2020	Coarse fine and filler fractions of RCA in SDA replaced at 50 and 100% of the fraction mass.	Water sensitivity, IT strength, rutting.
Laboratory study on recycled concrete aggregate based asphalt mixtures for sustainable flexible pavement surfacing	Nwakaire et al.	2020	Replacement of coarse and fine fractions in HMA at 20–100%.	Impact loading, stability, resilient modulus, IT strength, water sensitivity, fatigue, rutting, skid resistance, abrasion.
An interlaboratory test program on the extensive use of waste aggregates in asphalt mixtures: preliminary steps	Pasetto et al.	2020	RCA replacement in various mixtures.	Stability, water sensitivity.
Use of waste polyethylene for modification of bituminous paving mixes containing recycled concrete aggregates	Prakash Giri et al.	2020	RCA in HMA with plastic modified binder.	Stability, flow, IT strength, rutting.
Influence of recycled concrete aggregates from different sources in hot mix asphalt design	Sanchez-Cotte et al.	2020	Replacement of coarse fraction in HMA by RCA and C&D aggregates at 25, 30 and 45% replacement.	Resilient modulus, IT strength, water sensitivity.
Influence factors on using recycled concrete aggregate in foamed asphalt mixtures based on tensile strength and moisture resistance	Zou et al.	2020	RCA replaced at 25–100% in foamed asphalt mixtures.	IT strength, water sensitivity.
Investigation on the properties of aggregate-mastic interfacial transition zones (ITZs) in asphalt mixture containing recycled concrete aggregate	Huang et al.	2021	Study of the interfacial transition zone within asphalt mastic containing RCA.	Microscopy, adhesion.
Mechanical Performance of Gilsonite Modified Asphalt Mixture Containing Recycled Concrete Aggregate	Zuluaga-Astudillo et al.	2021	RCA replacement in HMA at 21 ad 24%.	Stability, resilient modulus, fatigue, IT strength, rutting.

2. Materials and methods

The materials employed in this study and the test methods are described in the following sections.

2.1. Materials

2.1.1. Binder and aggregates

The asphalt binder was an SBS (styrene-butadiene-styrene) polymer

modified binder (PmB) graded at 45/80–65 according to EN 1426, with PmB being a requirement for SDA in Switzerland (SN 640 436). The control aggregates were quarried sandstone with a 25–30% quartz content (from Massongex, Switzerland). The RCA was waste concrete from the Canton of Zurich region, stored at a concrete plant in Hinwil, Switzerland. The RCA was sieved into the fractions of 2/4, 0.125/2 and 0/0.125 mm, corresponding to the 2/4 mm (coarse), 0.063/4 mm (sand) and filler fractions of the control aggregates, respectively. Both of the 2/4 aggregates were also washed to removed loose dust/dirt particles and improve adhesion to bitumen in the mixtures. The apparent and relative aggregate densities were determined by EN 1097–6 (by gas pycnometer for the fillers) along with the sand equivalent (EN 933–8) and flow indices (EN 933–6) for the sand, as shown in Table 2. Due to the presence of cement paste, the bulk densities of the RCA were significantly lower than for the control aggregates, especially with regard to the coarse aggregates, consistent with what has been found with RCA (Ma et al., 2019; Pasetto et al., 2020). The water absorption is much more for the RCA coarse and sand compared to the control, as is expected from the densities and reported in the literature (Lei et al., 2020b). The absorption for the coarse RCA is higher than for the RCA sand, likely due to the fact that more of the coarse fraction has more absorptive cement attached.

The sand equivalent of the RCA was higher, due to the fact that the RCA sand was sieved in the lab while the control sand came from plant production conditions, where more fine materials could be present. The flow coefficients of the RCA sand was slightly higher than the control, and both were higher than the sand flow standard material of 32 s, meaning that the sands were angular (Sengoz et al., 2014).

2.1.2. Asphalt mixtures

The asphalt mixture was Semi-Dense Asphalt (SDA 4–16), a commonly used gap graded mixture in Switzerland for low noise pavements (Mikhailenko et al., 2020b). The maximum aggregate size was 4 mm and the required air voids content was 16 ± 2% (SN 640 436). The RCA were used to replace the control aggregates by volume based on the aggregate densities; the mix designs are shown by mass in Table 3.

Based on promising previous results in the literature described previously (Mikhailenko et al., 2020a; Piao et al., 2021), RCA filler was used for all RCA mixtures. The coarse (C) and sand (S) fractions replaced at about 15% of the mixture in separate mixtures, with two different binder contents for each replacement, resulting in over 20% RCA replacement in each mixture (Table 3). The binder content was 6.1% for the control mixtures, while the RCA mixtures had equivalent binder contents of 6.1 and 6.7% respectively, adjusted based on the estimated-Superpave binder absorption (McGennis et al., 1995) found previously for the same aggregates. It was shown that the binder absorption was insignificant for the RCA sand and estimated at 0.7% for 15% RCA 2/4 replacement from a previous study looking at RCA mixture binder absorption with the same aggregates (Mikhailenko et al., 2020a). Multiple binder contents were used with each RCA gradation to observe whether some of the potential weaknesses in RCA can be compensated for by increasing the binder.

Table 2
Physical properties of control virgin and recycled concrete aggregates.

Aggregate Fraction	Apparent Density (kg/m^3)	Bulk Density (kg/m^3)	Water Abs. 24 h (%)	Sand Eq. (%)	Flow Coeff. (s)
	EN 1097-6			EN 933-8	EN 933-6
FAMSA Filler	2729.3 [a]	–	–	–	–
FAMSA 0.063/4	2698.6	2657.4	0.57	54	35.7
FAMSA 2/4	2710.7	2647.0	0.89	–	–
RCA 0/0.125	2617.0 [a]	–	–	–	–
RCA 0.125/2	2654.4	2439.2	3.32	89	35.0
RCA 2/4	2609.3	2297.4	5.20	–	–

[a] Determined by gas pycnometer.

2.2. Methods

An overview of the experimental plan is given in Fig. 1, showing that aggregate characterization, mixture design and performance evaluation the main focus of the work. The binder and aggregates were heated to 170 °C before mixing. The aggregates were added to the drum first and mixed for 4 min, followed by the addition of the binder and filler and another 4 min of mixing. The maximum relative density of the loose mixture was determined by EN 12697–5 from three samples. The bulk density and air void content of all the samples was determined geometrically according to EN 12697-29 due to the higher voids content preventing the samples having a stable saturated surface dry condition during conventional density measurement.

The compactibility of the asphalt mixture was defined by a version of the Compaction Energy Index, CEI (Bahia et al., 1998) adapted later to mixtures with high air voids where the index was determined by taking the area of the compaction percentage (G_{mm}%) from the 8th gyration to 82% G_{mm} (Goh and You, 2012), with G_{mm} being the maximum theoretical specific gravity (Fig. 2). While the CEI should not be used to compare mixtures with different compaction temperatures, it is otherwise valid for comparing mixtures with local changes in the materials.

The low-temperature cracking resistance of the asphalt mixtures was determined according to the semi-circular bending (SCB) test EN 12697–44. The six cylindrical samples per mixture were compacted by gyratory compaction to a height of 50 mm and a diameter of 150 mm. Thereafter, the gyratory compacted samples were diamond saw cut on the top and bottom, reducing the height of each sample to 30 ± 3 mm. The samples were cut in half and a notch 10 ± 1 mm deep and 3.5 ± 1 mm wide was cut into the middle of each half. The sample was then subjected to three point loading at 0 °C at a vertical deformation rate of 5.0 ± 0.2 mm/min (EN 12697–44). From this, the fracture toughness, K_C, and the Fracture Energy (FE) can be calculated. The FE is derived by taking the area under the stress-displacement loading curve up to the peak (Fig. 3), while K_{Ic} (in N/m$^{3/2}$) is derived from the peak-stress σ_{max}, as in Eq. (1),

$$\sigma_{max} = \frac{4.263\ F_{max}}{D \times t} \quad (1)$$

where F_{max} is the peak load, D is the diameter of the specimen and t is the thickness. This can be used to compute Eq. (2) as follows:

$$K_{Ic} = \sigma_{max} f\left(\frac{a}{W}\right) \quad (2)$$

where $f\left(\frac{a}{W}\right)$ is a parameter incorporating the specimen height (W) and notch depth (a).

The rutting resistance of the mixtures was characterized by the Wheel Tracking Test (WTT) according to EN 12697–22. The test assesses the susceptibility of asphalt mixtures to deform by repeated passes of a loaded wheel at constant temperature of 60 °C. Two samples with dimensions 500 × 180 × 50 mm were compacted to the required air voids content, for each mixture using a steel wheel. Two sample from each mixture loaded with a solid rubber and treadless tire, with a diameter of 200 mm and a rectangular cross profile with a width of 50 ± 5 mm, for 30 000 passes, where each cycle consists of two passes (outward and return) of the loaded wheel. The mean rut depth was calculated using the recorded rut depth at 15 locations on the two samples. The wheel tracking rate is calculated as the slope of the rut depth between 10 000 and 3000 passes as in Eq. (3):

$$WTS = \frac{D_{10k} - D_{3k}}{7} \quad (3)$$

Table 3
SDA 4 mixture composition by mass.

Mixture Type	Code	Control Fraction %			RCA Fraction %			Binder %
		2/4	0.125/4	Filler	2/4	0.125/2	0/0.125	PmB 45/80–65
Control SDA 4	Cont	62.8	23.8	7.2	–	–	–	6.1
RCA 2/4 6.8%	6.8C	47.8	23.9	–	14.6	–	7.0	6.8
RCA 2/4 7.3%	7.3C	47.5	23.8	–	14.5	–	6.9	7.3
RCA 0.125/2 6.1%	6.1 S	63.4	8.9	–	–	14.9	7.0	6.1
RCA 0.125/2 6.7%	6.7 S	63.0	8.9	–	–	14.8	7.0	6.7

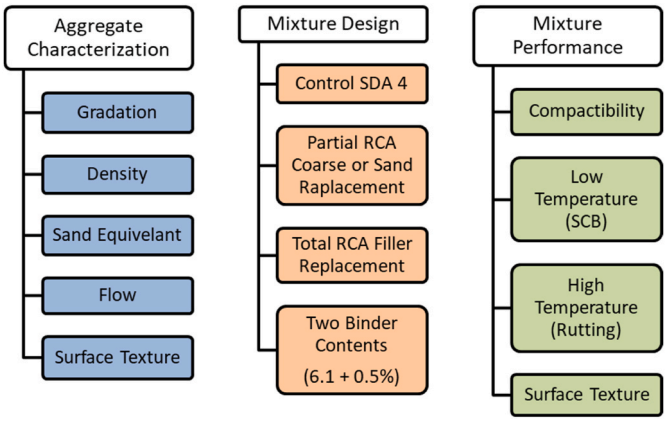

Fig. 1. Overview of experimental plan.

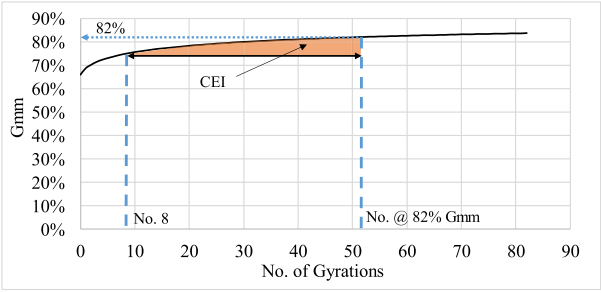

Fig. 2. Modified compaction energy index (CEI in G_{mm}*N) at 82% G_{mm} (Mikhailenko et al., 2020a).

where, *WTS* is the wheel-tracking slope, in millimeters per 10^3 load cycles, D_{3k}, D_{10k} is the rut depth (mm) after 3000 load cycles and 10 000 load cycles, respectively. The result of the test is the average WTS of two specimens.

The surface texture of the asphalt mixture samples was measured with an Ames Engineering 9400HD 3D laser scanner. The test was conducted on the rutting samples described previously, with a 100 × 50 mm surface scanned for pre-test samples and a 100 × 25 mm surface scanned in the middle of the wheel path for the post-rutting samples (Fig. 4). The resolutions were 0.005 mm vertically, 0.006 mm along the length of the scan (along the wheel path) and 0.025 mm for the width. A total of 250 scan lines were conducted for each area scan and used to calculate the average mean profile depth (MPD), skewness (R_{sk}) and kurtosis (R_{ku}), with four scans for each mixture-wheel path position. The MPD, an indicator of texture amplitude, was calculated removing wavelengths below 2.5 mm as prescribed by ISO 13473–1. Skewness can be positive or negative, with negative texture (<0) indicating lower vibration, possibly resulting in lower noise generation (Angst et al., 2016). Kurtosis is an indication of the surface jaggedness/roundness of the surface, with <3 indicating more roundedness (Li et al., 2016), and possibly being an indication of wear.

The texture level ($L_{TX,\lambda}$) relative to the texture wavelengths, λ, is calculated by taking the 1/3rd octave band power spectral density (PSD) graphs for every 10 scanlines and using Eq. (4) derived from ISO 13473–4.

$$L_{TX,\lambda} = 10\log\left(\frac{Z_{p,\lambda}{}^{*}0.232f}{a_{ref}^2}\right) dB \quad (4)$$

where $Z_{p,\lambda}$ is the 1/3rd octave band PSD amplitude for a certain texture bandwidth, λ, 0.232f represents the frequency corresponding to the bandwidth, and a_{ref} is the reference value of the surface profile amplitude (10^{-6} m given by ISO 13473–4). L_{TX} was found for texture wavelengths of 0.05–100 mm. ISO 13473–4 advises that the maximum texture wavelength analyzed, λ_{max} be much smaller than the analysis length, l, whereas in our case, $\lambda_{max} = l$. Given that ISO 13473–4 is written for laser scanners pulled by a car driving on the road, the long length is easier to come by than with laboratory samples.

This analysis was also conducted on the 2/4 mm aggregates to compare their surface roughness. The aggregate samples were placed in one layer on a 10 × 10 mm surface (Fig. 5). The laser scan was then conducted as described below for two samples for each aggregate, with

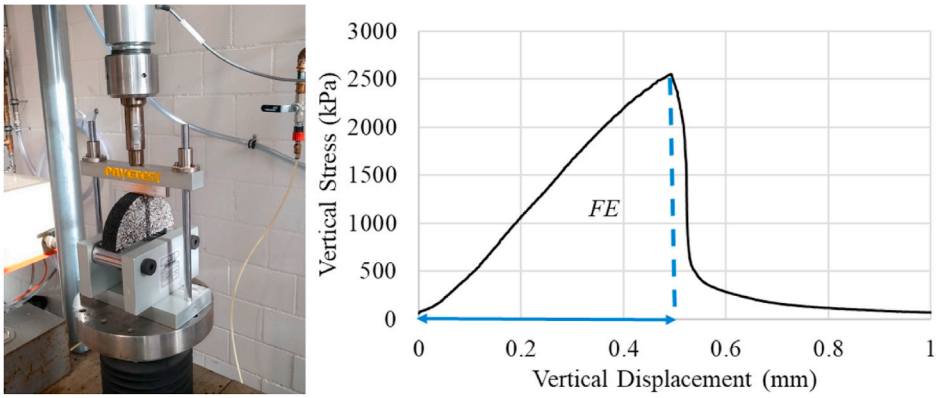

Fig. 3. Semi Circular Bending (SCB) testing (left) and calculation of fracture energy (right).

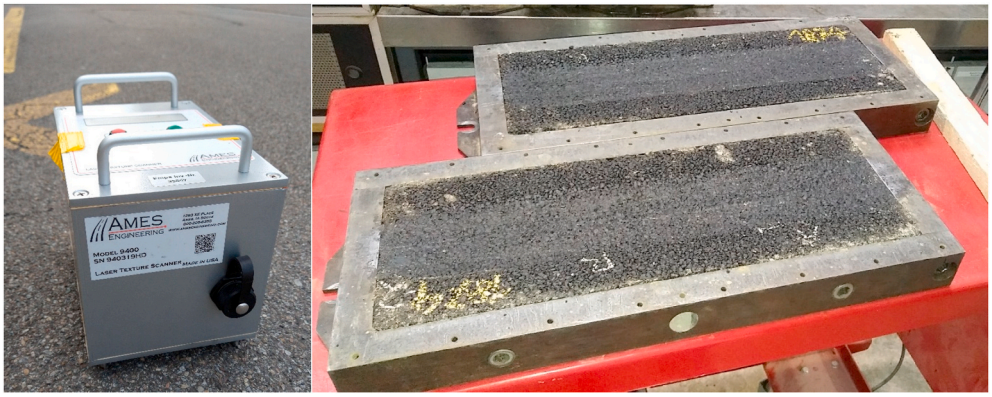

Fig. 4. Scanning asphalt texture with Ames Engineering 9400HD 3D laser scanner (left) and rutting sample after loading (right).

40 scan lines/mm and the microtexture level for wavelength (0.05–0.5 mm) of both was compared. Only the texture below 0.5 mm was considered in order to assess the surface of the aggregates as opposed to the caverns between aggregates.

In order to understand the performance of the RCA mixtures at a microscopic scale, one of the mixtures was subject to Scanning Electron Microscope (ESEM) analysis. This was done by cutting, impregnating with epoxy resin and polishing a 50 × 30 × 10 mm sample of the mixture and observing it with a FEI Quanta 650 ESEM at 50x magnification and 10 keV. A detailed description of this methodology can be found in (Poulikakos and Partl, 2010).

3. Results

The results of the study and relevant discussions will be described in the following sections.

3.1. Volumetrics and compactibility

The volumetric properties of the mixtures are calculated based on the Superpave methods (McGennis et al., 1995) and shown in Table 4. The RCA mixtures have lower bulk and maximum densities, which correspond to the lower density for the RCA. The voids in mineral aggregate (VMA) refers to the intergranular void space, which is the part of the effective binder (Eff. Binder in Table 4) and air voids combination that "participates" in the properties of the mixture as a percentage of the mixture volume. In contrast, the absorbed binder would be the binder absorbed in the surface voids of the aggregates (Sengoz and Topal, 2007). The VMA decreases somewhat with volume RCA replacement but increases with additional binder. The voids filled with asphalt (VFA), which is the percent intergranular voids filled with asphalt, increases with more binder as expected. The estimated effective binder content indicates that the amount of binder absorbed by RCA 2/4 was reasonably estimated and the effective binder content of sample 6.8C was very close to that of the control. However, the two binder contents for the RCA 2/4 mixtures ended up being 0.3% apart compared to 0.6% for the mixtures with RCA 0.125/2, which means the results may be closer for these samples.

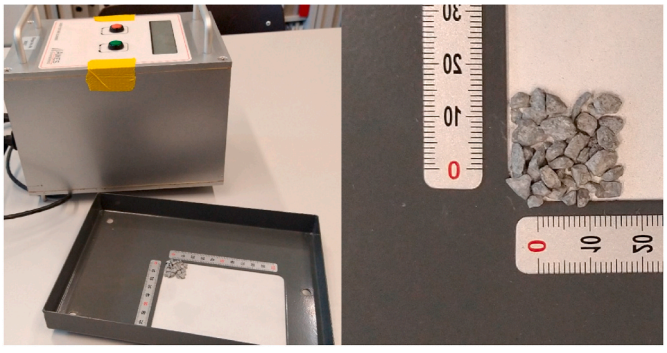

Fig. 5. Scanning coarse aggregate texture with Ames Engineering 9400HD 3D laser scanner.

The compactibility of the mixtures are shown in Fig. 6, with the number of gyrations and CEI matching fairly well. The mixtures with coarse RCA replacement are somewhat more difficult to compact than the control. Given that the effective binder contents are similar (Table 4), this would indicate that there may be intergranular locking or surface roughness in the coarse RCA compared with the control aggregates (Stakston et al., 2002). In the mixtures with fine RCA replacement, the higher binder content facilitated compaction.

3.2. Resistance to cracking by semi-circular bending

The SCB results are shown in Fig. 7, where it is clear that RCA replacement reduces the cracking resistance for the mixtures at 0 °C. The principal reason can be seen in the images of the fracture surfaces of the samples (Fig. 8), which show fractured aggregate surfaces. These are more easily seen in the RCA 2/4 but they are present for both cases of RCA replacement and not for the control. Although the fracture energy for both coarse and fine replacement are similar, the toughness for the coarse RCA mixtures are around 10% higher, indicating slightly better fracture performance. In addition, the different binder contents had no effect on the fracture performance at 0 °C in this case as the composite material is acting as a rigid solid at this temperature and the viscoelastic effect of the binder is minimal.

3.3. Wheel track rutting resistance

The wheel track testing results are show in Table 5 and Fig. 9. The rutting % at 30 000 cycles is similar to the control and almost within the standard deviation for coarse RCA samples with both binder contents. The samples with RCA sand however, have lower rutting damage than the control, especially for the sample where the binder content is 6.1%. The slope of the rutting (WTS) however, shows a higher slope for the control than all of the RCA samples, with the slopes for RCA coarse replacement being the lowest.

3.4. Surface texture

The surface texture parameters attained from the texture scanning are shown in Table 6, including the mean profile depth (MPD), skewness (R_{sk}) and kurtosis (R_{ku}). Additionally, the % difference is shown between the control and RCA samples, before and after 30 000 cycles of rutting and the % difference of the RCA samples from the control post-rutting.

Table 4
Superpave volumetric properties of asphalt mixtures including maximum and bulk density, air voids %, voids % in mineral aggregate (VMA) and filled with asphalt (VFA), along with the absorbed and effective binder %.

Sample	RCA%	Max. Density (kg/m^3)	Bulk Density (kg/m^3)	Air Voids %	VMA %	VFA %	Binder Added %	Abs. Binder %	Eff. Binder %
		EN 12697-5	EN 12697-29	EN 12697-5					
Control	0	2463.3	2061.9	16.3	27.1	39.8	6.1	0.8	5.4
Std Dev		*20.9*	*9.2*	*0.4*	*0.3*	*0.7*			
6.8C	21.6	2424.6	2053.5	15.3	25.9	41.0	6.8	1.5	5.3
Std Dev		*9.4*	*7.6*	*0.3*	*0.3*	*0.6*			
7.3C	21.4	2418.8	2035.3	15.9	27.0	41.3	7.3	1.7	5.6
Std Dev		*8.1*	*19.5*	*0.8*	*0.7*	*1.4*			
6.1 S	21.9	2438.7	2056.4	15.7	26.1	39.9	6.1	1.0	5.2
Std Dev		*7.5*	*9.5*	*0.4*	*0.3*	*0.7*			
6.7 S	21.7	2420.1	2039.6	15.7	27.1	41.9	6.7	1.0	5.7
Std Dev		*8.4*	*5.4*	*0.2*	*0.2*	*0.4*			

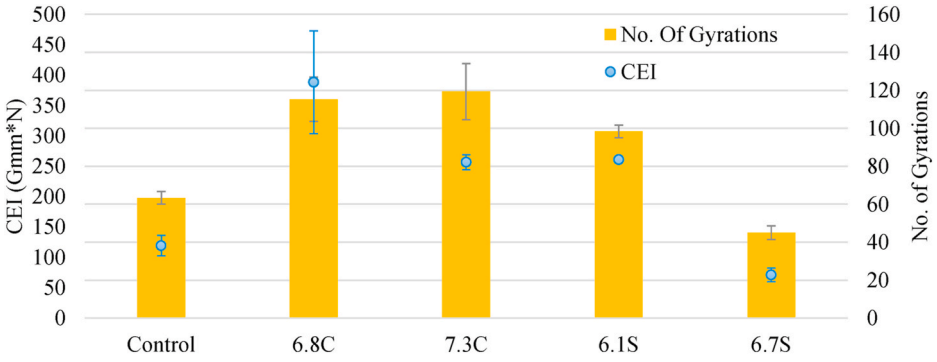

Fig. 6. Compactibility of asphalt mixtures based on modified compaction energy index (CEI) and no. of compactions.

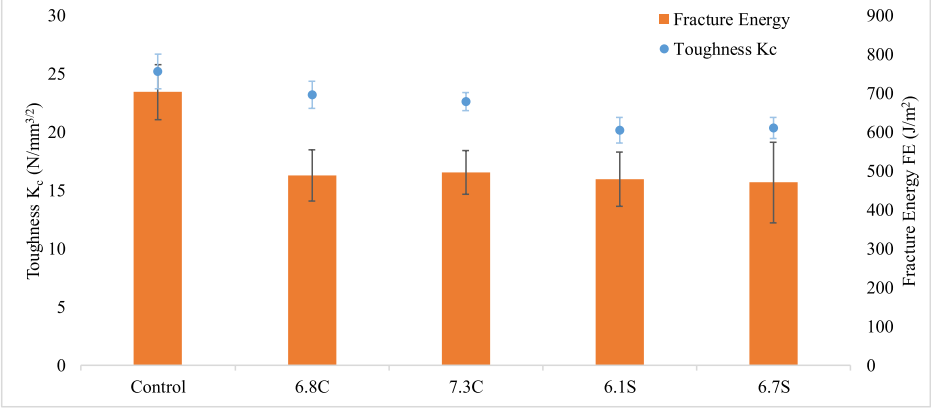

Fig. 7. Fracture energy and toughness from semi-circular bending test at 0 °C.

The MPD values are about the same as the control sample for the RCA coarse replacement, while being lower with RCA sand replacement. The texture skewness was similar for all of the samples at around −1.5 while the kurtosis was lower for the RCA samples, indicating the surface was somewhat more rounded.

When looking at the post-rutting samples, all of the samples had the same trend of MPD reducing in amplitude, the skewness showing more negative texture, while the kurtosis showed the trend toward more round texture. When comparing the effects of the wheel tracking on the samples, the response of the RCA samples differed depending on the effective binder (Table 4). The samples with the same effective binder to the control showed similar MPD amplitude, more positive texture and the control was made significantly more rounded than for the RCA samples (R_{ku}<3).

The texture level (L_{TX}) comparisons for the RCA samples are shown in Figs. 10 and 11. The texture level is reduced with RCA replacement, notably in the microtexture below 0.5 mm for RCA sand. The texture level is reduced in the post-rutting wheel path, especially below 5 mm, with a loss of 10 dB at 0.1 mm. Here, the microtexture is slightly better for the 6.7C samples compared to the control, while being about the same for the samples with RCA sand replacement.

To understand the difference in compactibility found previously, the coarse aggregates for the control and RCA were subject to laser texture scanning. As shown in Fig. 12, the microtexture level of the RCA 2/4 mm is about 1.5–2 dB higher than for the control, indicating a rougher surface.

3.5. Microscopic imaging

The microstructure of the 6.8C and 6.7 S samples were examined

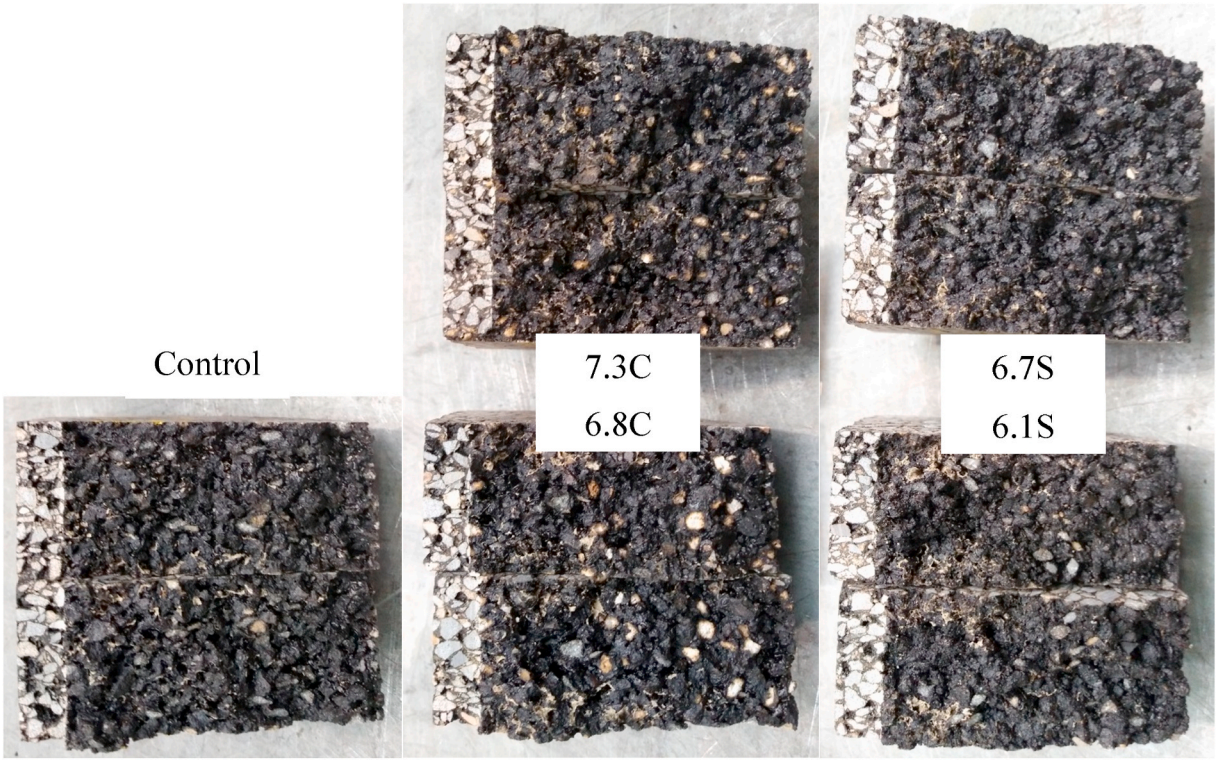

Fig. 8. Fracture surfaces of SCB samples (ø150 mm), where the white and grey particles show broken RCA.

Table 5
Properties and results of wheel tracking test samples.

Sample	Bulk Density (kg/m^3)	Air Voids %	% Rutting after 30 000 passes	WTS (mm)
Control	2097.3	14.9	6.90	0.078
Std Dev	*5.0*	*0.2*	*0.27*	*0.004*
6.8C	2047.8	16.0	6.95	0.053
Std Dev	*10.6*	*0.4*	*0.35*	*0.001*
7.3C	2033.0	15.6	6.41	0.050
Std Dev	*2.8*	*0.1*	*0.39*	*0.002*
6.1 S	2084.4	14.9	4.92	0.061
Std Dev	*1.7*	*0.1*	*0.05*	*0.004*
6.7 S	2082.5	14.4	6.02	0.070
Std Dev	*5.9*	*0.2*	*0.10*	*0.000*

with ESEM analysis. The image (Figs. 13 and 14) shows examples of the coarse and sand RCA sitting in the bitumen matrix and allows comparison of the two types of aggregates side by side showing that the microstructure of the two types of aggregates are different and can be clearly distinguished. Due to the fact that it is a composite material of aggregate and cement, it looks somewhat more rough than the sandstone sand, which may explain the higher compaction energy required for this mixture. The RCA is embedded in the asphalt mastic with no clear separation or adhesive failures.

4. Discussion

The replacement of sandstone aggregates with RCA at 20%w of SDA mixtures showed some potential and challenges. The required compaction for the same air voids content showed that while having the same

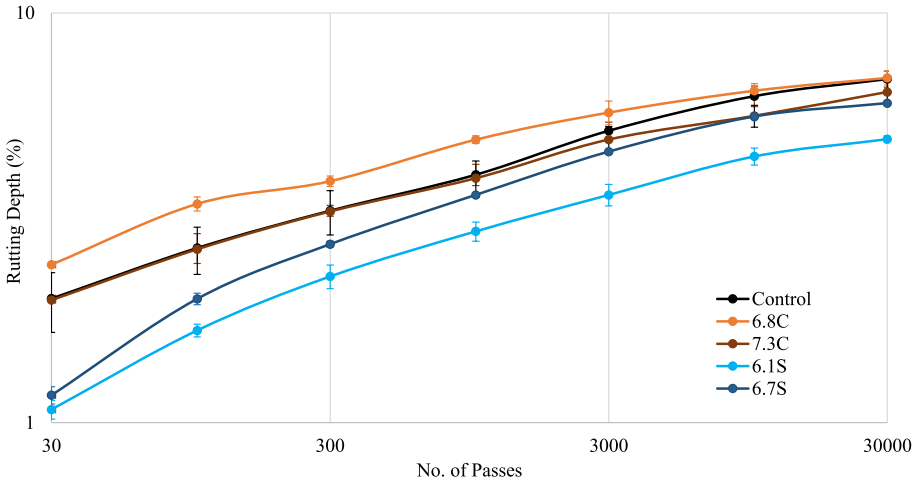

Fig. 9. rutting depth vs of number of passes from wheel tracking test.

Table 6
Texture parameters from laser texture scanning of samples before and asphalt wheel track testing.

Sample	Air Voids %	After Compaction (mm)			%Δ from Control			%Δ Post-Rutting			%Δ from Control Post-Rutting		
		MPD	R_{sk}	R_{ku}	MPD	R_{sk}	R_{ku}	MPD	R_{sk}	R_{ku}	MPD	R_{sk}	R_{ku}
Control	14.9	0.699	−1.565	3.277	–	–	–	+12.7	−90.7	−95.0	–	–	–
Std Dev	*0.2*	*0.056*	*0.063*	*0.346*									
6.8C	16.0	0.693	−1.520	2.822	−0.7	−2.9	−13.9	+10.1	−80.0	−56.6	−3.0	+108.9	+642.8
Std Dev	*0.4*	*0.029*	*0.050*	*0.256*									
7.3C	15.6	0.693	−1.503	2.776	−0.7	−3.9	−15.3	+20.6	−104.6	−115.4	+6.3	−147.4	−359.1
Std Dev	*0.1*	*0.034*	*0.054*	*0.202*									
6.1 S	14.9	0.542	−1.568	3.107	−22.4	+0.2	−5.2	+28.0	−82.1	−77.7	−11.9	+92.4	+319.0
Std Dev	*0.1*	*0.035*	*0.093*	*0.375*									
6.7 S	14.4	0.647	−1.509	2.690	−7.4	−3.6	−17.9	+10.8	−95.3	−101.7	−9.0	−50.9	−127.9
Std Dev	*0.2*	*0.034*	*0.075*	*0.422*									

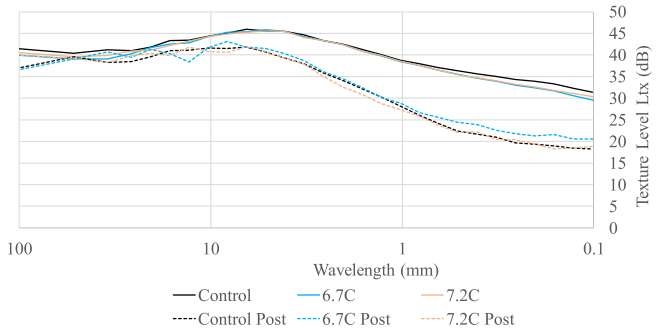

Fig. 10. Texture levels for coarse RCA replacement samples compared to control before and after (Post) wheel track loading.

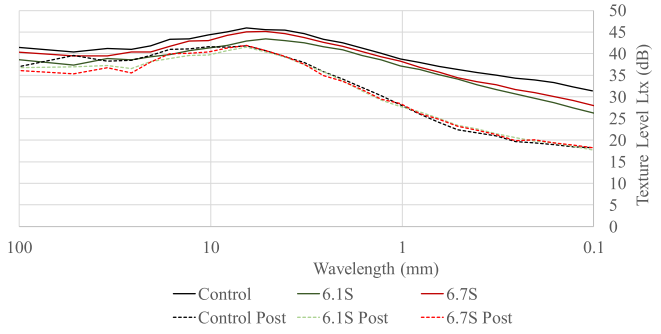

Fig. 11. Texture levels for sand RCA replacement samples compared to control before and after (Post) wheel track loading.

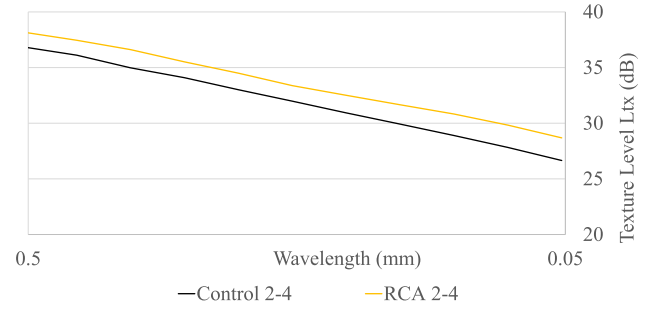

Fig. 12. Microtexture levels for coarse aggregates.

estimated effective binder content, the RCA mixtures were still more difficult to compact (Mikhailenko et al., 2020a), possibly due to more aggregate angularity or a rougher surface found in the texture scanning

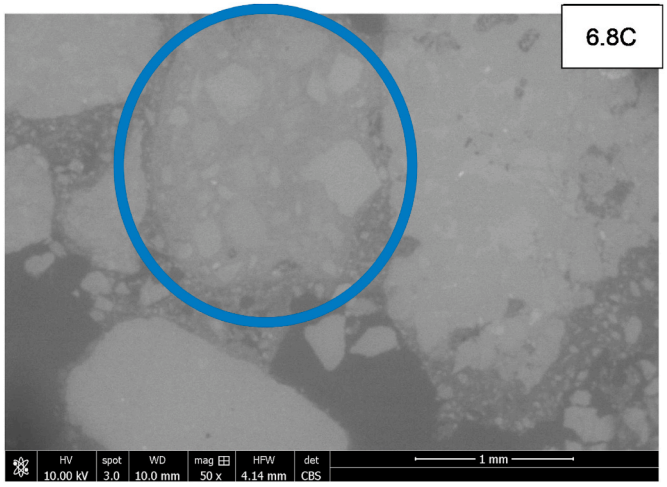

Fig. 13. Environmental scanning electron microscope (ESEM) images of the 6.8C sample, highlighting an RCA coarse aggregate just over 2 mm.

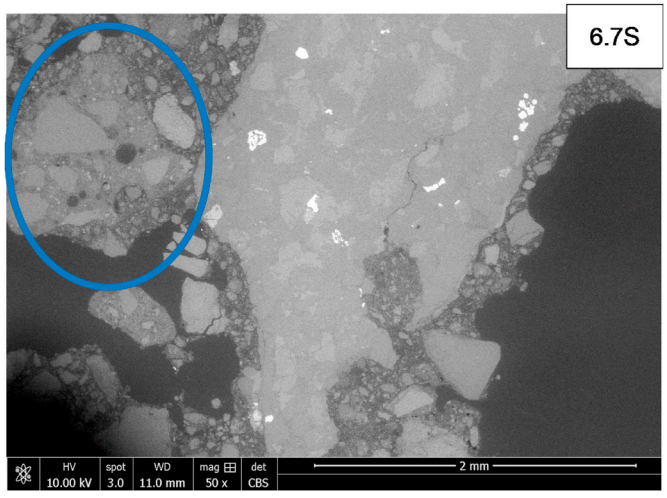

Fig. 14. Environmental scanning electron microscope (ESEM) images of the 6.7 S sample, highlighting an RCA sand aggregate just under 2 mm.

(Fig. 12). This difficulty was resolved by 0.5% extra binder in the RCA sand mixture where it achieved similar compactibility to the control (Fig. 6), but not for the RCA coarse mixtures.

A weakness for RCA mixture is cracking resistance due to the brittleness of the recycled aggregates leading to cohesive failure (Hou et al., 2014; Prakash Giri et al., 2020), and this was the case for 0 °C SCB testing of SDA with RCA replacement. This weakness has been

connected to the weakness in the interfacial transition zone between the cement paste and original aggregate within the RCA (Huang et al., 2021). The extra 0.5% binder did not have an effect on this due to the bitumen tending more brittle at 0 °C. This is sometimes mitigated by the addition of fibers when RCA is used in Portland cement concrete (Lei et al., 2020a).

The result was different with the EN 12697-44 measure of fracture toughness, based on the maximum stress, compared to the fracture energy based on the stress-strain curve. The RCA sand samples had 80% of the control fracture toughness in the control compared to 90% for the RCA coarse. This showed that despite the promising results (Arabani et al., 2013; Chen et al., 2011) of RCA sand in other studies (Mikhailenko et al., 2020a; Wu et al., 2013), RCA do not automatically become better performing as the size gets smaller and the trend is not linear. The SCB fracture toughness at 0 °C has correlated well to the low-temperature cracking shown by the thermal stress restrained specimen test (TSRST) (Zaumanis and Valters, 2018) and freeze-thaw splitting (Zhang et al., 2016). The SCB fracture energy in this case had high variability and this analysis may not apply well to these test conditions.

The rutting depth of the mixtures was not significantly affected by the coarse RCA replacement and reduced with RCA sand replacement. Given that the absorbed binder was accounted for, this is an indication that the shape of the RCA sand with higher angularity could have had provided more interlocking, as also indicated by the flow coefficient being somewhat lower (Table 2). The WTS results showed a lower slope for both RCA types with the same effective binder %, and especially lower in comparison to the control, indicating a slower rate of increase in rut depth with RCA replacement.

The texture level for the RCA mixtures seem to show a somewhat lower texture amplitude with RCA replacement, in terms of MPD (for the RCA sand) and L_{TX}. This could be a result of the somewhat higher compaction needed to achieve the required air voids content during compaction (Fig. 6). The lower texture in the macrotexture range has been correlated with lower noise (Del Pizzo et al., 2020; Losa et al., 2010), while lower microtexture has been correlated with lower skid-resistance (Ahammed and Tighe, 2010; Greer, 2006). The behavior of these mixtures' post-rutting is very similar in texture amplitude for the same binder content, with the L_{TX} not being very different in the wheel path for the different samples.

5. Conclusions and perspectives

This study aimed to replace virgin aggregates in low-noise SDA mixture with RCA at around 20% of the total mixture volume and evaluate the mixture properties in terms of volumetrics, compactibility, low-temperature cracking, rutting resistance and surface texture. This aimed to clarify the viability for RCA replacement in asphalt, which can reduce the amount of RCA waste going to landfills, while reducing the amount of virgin aggregates required in low-noise mixtures. The conclusions of this study are as follows:

- Volume replacement with RCA including compensation for binder absorption still lead to compactibility issues due to differences in the aggregate surface texture and shape.
- The low-temperature cracking resistance of the mixtures was lowered somewhat with RCA replacement, more with the RCA sand than with coarse. The increased binder content in the RCA mixtures did not have an effect on this property.
- The rutting resistance improved in mixtures with RCA replacement, due to the same aggregate surface roughness which affected the compaction.
- The texture level is reduced somewhat in mixtures with RCA replacement, suggesting possible lower skid resistance but this difference is negligible after wheel track testing surface wear.

While RCA replacement is promising for sustainability and improving the rutting resistance of low-noise asphalt, some properties such as low temperature cracking resistance are affected in a negative way, and would limit their use in surface mixtures such as SDA, where good cracking resistance is required. It is suggested by the authors that the focus could be on RCA filler replacement in the future, as opposed to the larger fractions. As for the coarse and fine fraction, they might be better candidates for lower asphalt layers where the performance requirements are not so stringent and the variability found in RCA less critical. It is also recommended that RCA asphalt and RCA production projects are connected to reduce this variability. Within the framework of this project, life cycle assessment and acoustic testing are also planned in order to quantify the environmental and health impacts.

Funding

The activity presented in this paper is part of Swiss National Science Foundation (SNF) grant 205121_178991/1 for the project titled "Urban Mining for Low Noise Urban Roads and Optimized Design of Street Canyons".

CRediT authorship contribution statement

Peter Mikhailenko: Conceptualization, Methodology, Investigation, Visualization, Writing – original draft, Writing – review & editing. **Zhengyin Piao:** Investigation, Writing – review & editing. **Muhammad Rafiq Kakar:** Investigation, Methodology, Writing – review & editing. **Moises Bueno:** Conceptualization, Writing – review & editing. **Lily D. Poulikakos:** Conceptualization, Writing – review & editing, Project administration, Funding acquisition.

Declaration of competing interest

The authors declare that they have no known competing financial interests or personal relationships that could have appeared to influence the work reported in this paper.

Acknowledgements

Thank you to the Empa Laboratory for Concrete and Asphalt technical staff for performing a part of the sample preparation and testing. Thank you to FAMSA (Massongex, Switzerland) for providing the asphalt mixture materials and FBB (Hinwil, Switzerland) for providing the RCA.

References

Acosta Alvarez, D., Alonso Aenlle, A., Tenza-Abril, A.J., 2018. Laboratory evaluation of hot asphalt concrete properties with Cuban recycled concrete aggregates. Sustainability 10, 2590. https://doi.org/10.3390/su10082590.

Acosta Álvarez, D., Alonso Aenlle, A., Tenza-Abril, A.J., Ivorra, S., 2020. Influence of partial coarse fraction substitution of natural aggregate by recycled concrete aggregate in hot asphalt mixtures. Sustainability 12, 250. https://doi.org/10.3390/su12010250.

Ahammed, M.A., Tighe, S.L., 2010. Pavement surface friction and noise: integration into the pavement management system. Can. J. Civ. Eng. 37, 1331–1340. https://doi.org/10.1139/L10-076.

Albayati, A., Wang, Yu, Wang, Yan, Haynes, J., 2018. A sustainable pavement concrete using warm mix asphalt and hydrated lime treated recycled concrete aggregates. Sustain. Mater. Technol. 18, e00081 https://doi.org/10.1016/j.susmat.2018.e00081.

Al-Bayati, H.K.A., Das, P.K., Tighe, S.L., Baaj, H., 2016. Evaluation of various treatment methods for enhancing the physical and morphological properties of coarse recycled concrete aggregate. Construct. Build. Mater. 112, 284–298. https://doi.org/10.1016/j.conbuildmat.2016.02.176.

Angst, C., Bürgisser, P., Beckenbauer, T., 2016. IMPACT: Investigation Machine for Pavement ACoustic durability; Testing the durability of low noise road. In: Proceedings of 6th Eurasphalt & Eurobitume Congress. Czech Technical University, Prague, Prague, Czech Republic. https://doi.org/10.14311/EE.2016.230.

Arabani, M., Nejad, F.M., Azarhoosh, A.R., 2013. Laboratory evaluation of recycled waste concrete into asphalt mixtures. Int. J. Pavement Eng. 14, 531–539. https://doi.org/10.1080/10298436.2012.747685.

Bahia, H.U., Friemel, T.P., Peterson, P.A., Russell, J.S., Poehnelt, B., 1998. Optimization of constructibility and resistance to traffic: a new design approach for HMA using the superpave compactor. J. Assoc. Asph. Paving Technol. 67.
Birgisson, B., Roberson, R., 2000. Drainage of pavement base material: design and construction issues. Transport. Res. Rec. 1709, 11–18. https://doi.org/10.3141/1709-02.
Bogas, J.A., de Brito, J., Ramos, D., 2016. Freeze–thaw resistance of concrete produced with fine recycled concrete aggregates. J. Clean. Prod. 115, 294–306. https://doi.org/10.1016/j.jclepro.2015.12.065.
Castillo, D., Caro, S., Darabi, M., Masad, E., 2018. Influence of aggregate morphology on the mechanical performance of asphalt mixtures. Road Mater. Pavement Des. 19, 972–991. https://doi.org/10.1080/14680629.2017.1283357.
Chen, M., Lin, J., Wu, S., 2011. Potential of recycled fine aggregates powder as filler in asphalt mixture. Construct. Build. Mater. 25, 3909–3914. https://doi.org/10.1016/j.conbuildmat.2011.04.022.
Chen, M.J., Wong, Y.D., 2013. Porous asphalt mixture with 100% recycled concrete aggregate. Road Mater. Pavement Des. 14, 921–932. https://doi.org/10.1080/14680629.2013.837839.
Del Pizzo, A., Teti, L., Moro, A., Bianco, F., Fredianelli, L., Licitra, G., 2020. Influence of texture on tyre road noise spectra in rubberized pavements. Appl. Acoust. 159, 107080. https://doi.org/10.1016/j.apacoust.2019.107080.
El-Tahan, D., Gabr, A., El-Badawy, S., Shetawy, M., 2018. Evaluation of recycled concrete aggregate in asphalt mixes. Innov. Infrastruct. Solut. 3, 20. https://doi.org/10.1007/s41062-018-0126-7.
EN 933-6, 2014. Tests for Geometrical Properties of Aggregates - Part 6: Assessment of Surface Characteristics - Flow Coefficient of Aggregates.
EN 933-8, 2012. Tests for Geometrical Properties of Aggregates Part 8: Assessment of Fines - Sand Equivalent Test.
EN 1097-6, 2013. Tests for Mechanical and Physical Properties of Aggregates - Part 6: Determination of Particle Density and Water Absorption.
EN 1426, 2015. Bitumen and Bituminous Binders. Determination of needle penetration.
EN 12697-5, 2019. Bituminous Mixtures - Test Methods - Part 5: Determination of the Maximum Density.
EN 12697-22, 2003. Bituminous Mixtures - Test Methods for Hot Mix Asphalt - Part 22: Wheel Tracking.
EN 12697-29, 2002. Bituminous Mixtures - Test Method for Hot Mix Asphalt - Part 29: Determination of the Dimensions of Bituminous Specimen.
EN 12697-44, 2019. Bituminous Mixtures - Test Methods for Hot Mix Asphalt - Part 44: Crack Propagation by Semi-circular Bending Test.
Gálvez-Martos, J.-L., Styles, D., Schoenberger, H., Zeschmar-Lahl, B., 2018. Construction and demolition waste best management practice in Europe. Resour. Conserv. Recycl. 136, 166–178. https://doi.org/10.1016/j.resconrec.2018.04.016.
Goh, S.W., You, Z., 2012. Mechanical properties of porous asphalt pavement materials with warm mix asphalt and RAP. J. Transport. Eng. 138, 90–97. https://doi.org/10.1061/(ASCE)TE.1943-5436.0000307.
Greer, G., 2006. Stone mastic asphalt-A review of its noise reducing and early life skid resistance properties. In: Proceedings of ACOUSTICS 2006, Christchurch, New Zealand, pp. 319–323.
Hou, Y., Ji, X., Su, X., Zhang, W., Liu, L., 2014. Laboratory investigations of activated recycled concrete aggregate for asphalt treated base. Construct. Build. Mater. 65, 535–542. https://doi.org/10.1016/j.conbuildmat.2014.04.115.
Huang, Q., Qian, Z., Hu, J., Zheng, D., Chen, L., Zhang, M., Yu, J., 2021. Investigation on the properties of aggregate-mastic interfacial transition zones (ITZs) in asphalt mixture containing recycled concrete aggregate. Construct. Build. Mater. 269, 121257. https://doi.org/10.1016/j.conbuildmat.2020.121257.
ISO 13473-1, 2019. Characterization of Pavement Texture by Use of Surface Profiles — Part 1: Determination of Mean Profile Depth.
ISO 13473-4, 2008. Characterization of Pavement Texture by Use of Surface Profiles — Part 4: Spectral Analysis of Surface Profiles.
Jacobs, M.M., van den Beemt, R.C., Frunt, M.H., 2015. Determination of the scuffing resistance of porous asphalt using annex A of prTS 12697-50 (the ARTe). In: International Conference on Bituminous Mixtures and Pavements, 6th, 2015, Thessaloniki, Greece.
Kareem, A.I., Nikraz, H., Asadi, H., 2019. Performance of hot-mix asphalt produced with double coated recycled concrete aggregates. Construct. Build. Mater. 205, 425–433. https://doi.org/10.1016/j.conbuildmat.2019.02.023.
Kareem, A.I., Nikraz, H., Asadi, H., 2018. Evaluation of the double coated recycled concrete aggregates for hot mix asphalt. Construct. Build. Mater. 172, 544–552. https://doi.org/10.1016/j.conbuildmat.2018.03.158.
Leemann, A., Loser, R., 2019. Carbonation resistance of recycled aggregate concrete. Construct. Build. Mater. 204, 335–341. https://doi.org/10.1016/j.conbuildmat.2019.01.162.
Lei, B., Li, W., Liu, H., Tang, Z., Tam, V.W.Y., 2020a. Synergistic effects of polypropylene and glass fiber on mechanical properties and durability of recycled aggregate concrete. Int. J. Concr. Struct. Mater. 14, 37. https://doi.org/10.1186/s40069-020-00411-2.
Lei, B., Li, W., Luo, Z., Tam, V.W.Y., Dong, W., Wang, K., 2020b. Performance enhancement of permeable asphalt mixtures with recycled aggregate for concrete pavement application. Front. Mater. https://doi.org/10.3389/fmats.2020.00253, 0.
Li, L., Wang, K.C.P., Li, Q., Joshua, 2016. Geometric texture indicators for safety on AC pavements with 1mm 3D laser texture data. Int. J. Pavement Res. Technol. 9, 49–62. https://doi.org/10.1016/j.ijprt.2016.01.004.
Losa, M., Leandri, P., Bacci, R., 2010. Empirical rolling noise prediction models based on pavement surface characteristics. Road Mater. Pavement Des. 11, 487–506. https://doi.org/10.1080/14680629.2010.9690343.
Ma, J., Sun, D., Pang, Q., Sun, G., Hu, M., Lu, T., 2019. Potential of recycled concrete aggregate pretreated with waste cooking oil residue for hot mix asphalt. J. Clean. Prod. 221, 469–479. https://doi.org/10.1016/j.jclepro.2019.02.256.
McGennis, R.B., Anderson, R.M., Kennedy, T.W., Solaimanian, M., 1995. Background of SUPERPAVE Asphalt Mixture Design and Analysis. Federal Highway Administration. Office of Technology Applications, United States.
Mikhailenko, P., Kakar, M.R., Piao, Z., Bueno, M., Poulikakos, L., 2020a. Incorporation of recycled concrete aggregate (RCA) fractions in semi-dense asphalt (SDA) pavements: volumetrics, durability and mechanical properties. Construct. Build. Mater. 264, 120166. https://doi.org/10.1016/j.conbuildmat.2020.120166.
Mikhailenko, P., Piao, Z., Kakar, M.R., Bueno, M., Athari, S., Pieren, R., Heutschi, K., Poulikakos, L., 2020b. Low-Noise pavement technologies and evaluation techniques: a literature review. Int. J. Pavement Eng. https://doi.org/10.1080/10298436.2020.1830091.
Mills-Beale, J., You, Z., 2010. The mechanical properties of asphalt mixtures with Recycled Concrete Aggregates. Construct. Build. Mater. 24, 230–235. https://doi.org/10.1016/j.conbuildmat.2009.08.046.
Monier, V., Mudgal, S., Hestin, M., Trarieux, M., Mimid, S., 2011. Service Contract on Management of Construction and Demolition Waste–SR1 Final Report Task 2. European Commission DG ENV.
Nejad, F.M., Azarhoosh, A.R., Hamedi, G.H., 2013. The effects of using recycled concrete on fatigue behavior of hot mix asphalt. J. Civ. Eng. Manag. 19, 61–68. https://doi.org/10.3846/13923730.2013.801892.
Nwakaire, C.M., Yap, S.P., Yuen, C.W., Onn, C.C., Koting, S., Babalghaith, A.M., 2020. Laboratory study on recycled concrete aggregate based asphalt mixtures for sustainable flexible pavement surfacing. J. Clean. Prod. 262, 121462. https://doi.org/10.1016/j.jclepro.2020.121462.
Orešković, M., Trifunović, S., Mladenović, G., 2019. Use of hydrated lime and cement bypass dust as alternative fillers in hot mix asphalt. In: 17th Colloquium Asphalt, Bitumen and Pavements, Bled, Slovenia.
Ossa, A., García, J.L., Botero, E., 2016. Use of recycled construction and demolition waste (CDW) aggregates: a sustainable alternative for the pavement construction industry. J. Clean. Prod. 135, 379–386. https://doi.org/10.1016/j.jclepro.2016.06.088.
Pasandín, A.R., Pérez, I., 2017. Fatigue performance of bituminous mixtures made with recycled concrete aggregates and waste tire rubber. Construct. Build. Mater. 157, 26–33. https://doi.org/10.1016/j.conbuildmat.2017.09.090.
Pasetto, M., Pasquini, E., Giacomello, G., Moreno-Navarro, F., Tauste-Martinez, R., Cannone Falchetto, A., Vaillancourt, M., Russo, F., Skaf, M., Orešković, M., Freire, A. C., Mikhailenko, P., Poulikakos, L., 2020. An interlaboratory test program on the extensive use of waste aggregates in asphalt mixtures: preliminary steps. In: Presented at the RILEM International Symposium on Bituminous Materials - ISBM 2020, Lyon, France.
Pérez Pérez, I., Gallego Medina, J., Toledano, M., Taibo Pose, J., 2010. Asphalt mixtures with construction and demolition debris. Proc. Inst. Civ. Eng.-Transp. 163, 165–174.
Piao, Z., Mikhailenko, P., Kakar, M.R., Bueno, M., Hellweg, S., Poulikakos, L.D., 2021. Urban mining for asphalt pavements: a review. J. Clean. Prod. 280, 124916. https://doi.org/10.1016/j.jclepro.2020.124916.
Poulikakos, L.D., Athari, S., Mikhailenko, P., Piao, Z., Kakar, M.R.K., Bueno, M., Pieren, R., Heutschi, K., 2019. Use of waste and marginal materials for silent roads. In: Proceedings of the 23rd International Congress on Acoustics, Aachen, Germany.
Poulikakos, L.D., Papadaskalopoulou, C., Hofko, B., Gschösser, F., Cannone Falchetto, A., Bueno, M., Arraigada, M., Sousa, J., Ruiz, R., Petit, C., Loizidou, M., Partl, M.N., 2017. Harvesting the unexplored potential of European waste materials for road construction. Resour. Conserv. Recycl. 116, 32–44. https://doi.org/10.1016/j.resconrec.2016.09.008.
Poulikakos, L.D., Partl, M.N., 2010. Investigation of porous asphalt microstructure using optical and electron microscopy. J. Microsc. 240, 145–154. https://doi.org/10.1111/j.1365-2818.2010.03388.x.
Prakash Giri, J., Panda, M., Sahoo, U.C., 2020. Use of waste polyethylene for modification of bituminous paving mixes containing recycled concrete aggregates. Road Mater. Pavement Des. 21, 289–309. https://doi.org/10.1080/14680629.2018.1487873.
Radević, A., Đureković, A., Zakić, D., Mladenović, G., 2017. Effects of recycled concrete aggregate on stiffness and rutting resistance of asphalt concrete. Construct. Build. Mater. 136, 386–393. https://doi.org/10.1016/j.conbuildmat.2017.01.043.
Riviera, P.P., Bellopede, R., Marini, P., Bassani, M., 2014. Performance-based re-use of tunnel muck as granular material for subgrade and sub-base formation in road construction. Tunn. Undergr. Space Technol. 40, 160–173. https://doi.org/10.1016/j.tust.2013.10.002.
Sadati, S., Khayat, K.H., 2018. Can concrete containing high-volume recycled concrete aggregate Be durable? ACI Mater. J. Farmington Hills 115, 471–480. https://doi.org/10.14359/51702190.
Sanchez-Cotte, E.H., Fuentes, L., Martinez-Arguelles, G., Rondón Quintana, H.A., Walubita, L.F., Cantero-Durango, J.M., 2020. Influence of recycled concrete aggregates from different sources in hot mix asphalt design. Construct. Build. Mater. 259, 120427. https://doi.org/10.1016/j.conbuildmat.2020.120427.
Sengoz, B., Onsori, A., Topal, A., 2014. Effect of aggregate shape on the surface properties of flexible pavement. KSCE J. Civ. Eng. 18, 1364–1371. https://doi.org/10.1007/s12205-014-0516-0.
Sengoz, B., Topal, A., 2007. Minimum voids in mineral aggregate in hot-mix asphalt based on asphalt film thickness. Build. Environ. 42, 3629–3635. https://doi.org/10.1016/j.buildenv.2006.10.005.
Soleimanbeigi, A., Shedivy, R.F., Tinjum, J.M., Edil, T.B., 2015. Climatic effect on resilient modulus of recycled unbound aggregates. Road Mater. Pavement Des. 16, 836–853. https://doi.org/10.1080/14680629.2015.1060250.

Stakston, A.D., Bahia, H.U., Bushek, J.J., 2002. Effect of fine aggregate angularity on compaction and shearing resistance of asphalt mixtures. Transport. Res. Rec. 1789, 14–24. https://doi.org/10.3141/1789-02.

Steiner, S., Bühlmann, E., Hammer, E., 2018. Milestones in establishing low-noise asphalts as a widely used, effective and durable noise abatement measure in Switzerland. In: Euronoise 2018. Presented at the Euronoise 2018, Crete, Greece.

Swiss Standard SN 640 436 Semidichtes Mischgut und Deckschichten Festlegungen, 2013. Anforderungen, Konzeption und Ausführung.

UEPG, 2018. Annual Review 2017-2018. European Aggregates Association, Brussels, Belgium.

Wu, S., Muhunthan, B., Wen, H., 2017. Investigation of effectiveness of prediction of fatigue life for hot mix asphalt blended with recycled concrete aggregate using monotonic fracture testing. Construct. Build. Mater. 131, 50–56. https://doi.org/10.1016/j.conbuildmat.2016.11.045.

Wu, S., Zhong, J., Zhu, J., Wang, D., 2013. Influence of demolition waste used as recycled aggregate on performance of asphalt mixture. Road Mater. Pavement Des. 14, 679–688. https://doi.org/10.1080/14680629.2013.779304.

Yaghoubi, E., Disfani, M.M., Arulrajah, A., Kodikara, J., 2018. Impact of compaction method on mechanical characteristics of unbound granular recycled materials. Road Mater. Pavement Des. 19, 912–934. https://doi.org/10.1080/14680629.2017.1283354.

Ye, G., van Breugel, K., Lura, P., Mechtcherine, V., 2012. Hardening process of binder paste and microstructure development. In: Mechtcherine, V., Reinhardt, H.-W. (Eds.), Application of Super Absorbent Polymers (SAP) in Concrete Construction: State-Of-The-Art Report Prepared by Technical Committee 225-SAP, RILEM State of the Art Reports. Springer Netherlands, Dordrecht, pp. 51–62. https://doi.org/10.1007/978-94-007-2733-5_6.

Zaumanis, M., Valters, A., 2018. Comparison of two low-temperature cracking tests for use in performance-based asphalt mixture design. Int. J. Pavement Eng. 1–9. https://doi.org/10.1080/10298436.2018.1549323, 0.

Zhang, Z., Wang, K., Liu, H., Deng, Z., 2016. Key performance properties of asphalt mixtures with recycled concrete aggregate from low strength concrete. Construct. Build. Mater. 126, 711–719. https://doi.org/10.1016/j.conbuildmat.2016.07.009.

Zou, G., Sun, X., Liu, X., Zhang, J., 2020. Influence factors on using recycled concrete aggregate in foamed asphalt mixtures based on tensile strength and moisture resistance. Construct. Build. Mater. 265, 120363. https://doi.org/10.1016/j.conbuildmat.2020.120363.

Zuluaga-Astudillo, D.A., Rondón-Quintana, H.A., Zafra-Mejía, C.A., 2021. Mechanical performance of gilsonite modified asphalt mixture containing recycled concrete aggregate. Appl. Sci. 11, 4409. https://doi.org/10.3390/app11104409.